ANALYTICAL SERIES

Fluorescence Decay Methods for the Characterization of Latex Film Formation

By **J.M.G. Martinho** and **J.P.S. Farinha**,
CQFM, Instituto Superior Tecnico

Fluorescence decay methods have been used extensively to characterize the formation of polymer films from latex dispersions, a process widely used in the coatings industry. By measuring the polymer chain diffusion at the nanometer scale, this technique enables the quantification of the amount of mixing between polymer particles that ultimately contributes to the formation of a polymer coating with good mechanical properties. This article provides an introduction to fluorescence decay methods, with a strong emphasis on their application to the characterization of latex film formation. Examples are also provided, demonstrating how this technique has been used to help in the understanding of this process in different latex coatings.

INTRODUCTION TO THE PROBLEM

Latex Film Formation

The different stages involved in the formation of a film from a water dispersion of polymer nanoparticles, or latex, are schematically shown in *Figure* 1.[1-4] After water evaporation and drying, the polymer particles form a densely close-packed arrangement. At temperatures above the "minimum film formation temperature" (MFFT, which is close to the glass transition temperature of the polymer in the presence of water), a transparent film is formed by deformation of the particles, through a combination of capillary, osmotic, and surface forces that overcome the elastic modulus of the particles.[1] To form a mechanically strong film, the polymer chains have to further diffuse across the interfaces between adjacent particles, in a process driven by the increase in entropy associated with the healing of these interfaces. This last stage is of utmost importance to the final properties of the film. Therefore, to modify coating formulations and design more efficient coatings, it is necessary to understand the characteristics of polymer diffusion for the particular formulation of interest.

Measuring Polymer Diffusion During Film Formation

The most commonly used techniques for studying polymer interdiffusion across the interface in latex film formation are small angle neutron scattering (SANS) and Förster resonance energy transfer (FRET). SANS experiments, first used by Hahn[5,6] to study the relation between polymer interdiffusion and film tensile strength,[7]

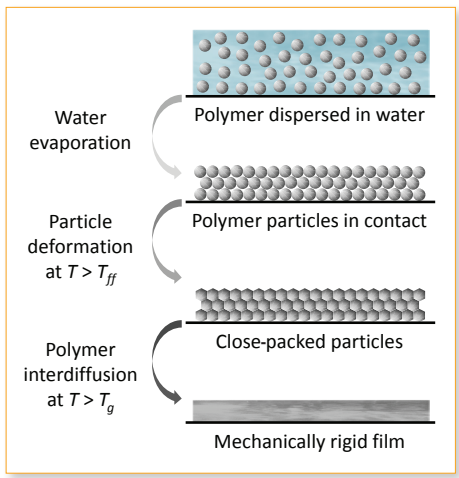

Figure 1—Formation of a film from a water dispersion of polymer nanoparticles.

require the preparation of deuterated and nondeuterated polymer particles to achieve contrast. The use of FRET to analyze polymer mixing, an approach pioneered by Morawetz[8-10] and extensively used by Winnik to study latex film formation,[11,12] requires the preparation of polymer particles labeled with a small amount (typically less than 1 mol%) of two different dyes: a fluorescent energy donor dye and an energy acceptor dye.[13] These dyes are usually incorporated into the latex particles via dye comonomers with appropriate polymerizable groups, such as methacrylate or vinyl substituents. FRET has been used to study the effects of different factors on latex film formation: temperature,[14] composition,[15] moisture,[16] coalescing aids,[3,17-19] polar groups at the latex surface,[20] the presence of filler particles, etc. [21-24]

The films are prepared from a blend of FRET donor- and acceptor-labeled latex particles, for which the fluorescence spectra of the donor overlaps the absorption spectra of the acceptor. Since the molar fraction of the dyes is very low, one can assume that the donor and acceptor dyes serve only as traces for the location of the polymer. The donor- and acceptor-labeled particles should, in principle, have similar size, as well as similar molecular weight and molecular weight distribution of their constituent polymers. This can be achieved by synthesizing both particles from a common unlabeled seed latex with a size much smaller than the final latex particles. To measure the fluorescence decay curve of the donor in the films, a pulse of light with a wavelength selectively absorbed by the donor dye is used. The donor decay is affected by nonradiative energy transfer to the acceptor dyes in proximity (typically a few nanometers to tens of nanometers, depending on the dyes), and this effect can be used as a "molecular ruler" to evaluate the donor-acceptor separation.

If donor and acceptor dyes are located in different particles, FRET measurements can be used to evaluate the extent of mixing during the formation of the polymer film. In the nascent film (obtained upon drying the latex dispersion), the dyes are confined to separate particles, and the efficiency of FRET is limited because it occurs only across the interface between adjacent particles. Subsequent curing of the film leads to polymer diffusion across the interface between particles, mixing of donor- and acceptor-labeled polymer chains, and a resultant increase in the efficiency of energy transfer. Although this effect can also be evaluated by following the decrease in fluorescence intensity of the donor spectra, this is subject to numerous artifacts, and therefore it is typical to measure instead the fluorescence decay of the donor. These experimental artifacts are related to geometrical and light scattering effects, as well as to the difficulty in assuring that the excitation energy is exclusively absorbed by the donor in the donor/acceptor-mixed films.

FÖRSTER RESONANCE ENERGY TRANSFER IN POLYMER COATINGS

Since the pioneering work of Morawetz,[8] the formalism of FRET has been developed to accommodate increasingly complex geometries[25-27] and dye distributions,[19,28-32] allowing the experimental determination of dye concentration profiles in complex nanostructured materials.[33]

To use FRET in the characterization of latex film formation, one mixes polymer particles labeled with a small amount (typically less than 1 mol%) of a fluorescent energy donor dye (D) with polymer particles labeled with an acceptor dye (A). After casting the film, this is irradiated with visible or UV radiation that should be mainly absorbed by D, and electronic energy can then be transferred to a nearby A by a resonance dipole–dipole coupling mechanism. The efficiency of FRET depends on the inverse six power of the D–A distance, in a length scale of a few nanometers (depending on the D–A pair used). The typical length scale of FRET matches the size of interparticle domains in latex films, and is small enough to avoid interference by capillary waves at the interface. In a typical experiment, two latex dispersions (one labeled with an energy donor and the other with an acceptor) are mixed. If the film is dried at about the glass transition temperature (T_g) of the polymers, FRET occurs only across the interfaces between D- and A-labeled neighboring particles. Annealing of the film above the T_g of the polymers leads to colocalization of the dyes in the interparticle regions, and one observes an increase in the quantum efficiency of energy transfer. Since the dye distribution mimics the distribution of the polymer components, these experiments can provide detailed information on the distribution of the labeled polymer components and the morphology of the nanostructure.[33]

EXPERIMENTAL SETUPS FOR FLUORESCENCE DECAY MEASUREMENT BY SINGLE-PHOTON TIMING

The most commonly used technique to record fluorescence decay curves is time-correlated single-photon counting (TCSPC), better designated as *single-photon timing* (SPT). *Figure* 2 shows a diagram of the modules that compose typical SPT equipment.[34]

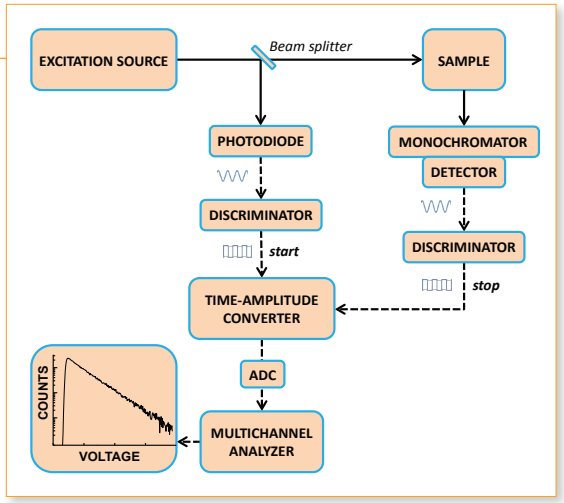

Figure 2—Equipment diagram for fluorescence decay time measurement by the single-photon timing (SPT) technique.

The heart of this technique is the time-to-amplitude converter (TAC) that translates the difference in time between two pulses to a voltage. The sample can be electronically excited using a pulsed lamp (nanosecond pulse width) or a pulsed laser (picosecond pulse width). An electric signal associated with the excitation pulse is generated (e.g., from the electronics of the excitation source or from a fast photodiode that detects a small fraction of the excitation light) and routed through a discriminator to initiate the TAC (*start* pulse). The *stop* signal is generated by the fluorescence of the sample, which is detected by a photomultiplier (preferably, a microchannel plate, which has faster response times and practically no "color effect"). The interval between the start and the stop signals is converted in an analog output pulse proportional to the time between these signals.

As the probability of detecting a single photon at time *t* after excitation is proportional to the fluorescence intensity, the histogram of the number of counts versus voltage reproduces the fluorescence decay curve. The TAC and the associated analog to digital converter (ADC) must guarantee a very good linearity in the full range of operating voltages. The TAC signals corresponding to valid start–stop cycles are stored in a multichannel analyzer (MCA) according to their voltage. The voltage is then converted in time by the calibration of the TAC, and the fluorescence decay curve is recorded.

The popularity and preeminence of the SPT technique stems from its high sensitivity, excellent dynamic range and linearity, and well-defined Poisson statistics. To ensure that a probability of detecting two fluorescence photons per excitation pulse is low, the number of fluorescence pulses have to be much smaller (ca. < 2%) than that of excitation pulses. To obtain the decay curve with good statistics, the number of counts at the maximum channel should be high (~20,000 counts).

This requires excitation sources delivering light pulses at high repetition rates. Thanks to pulsed lasers delivering pulses in the MHz range, fluorescence decays can be acquired in minutes. For high repetition rate sources, it is recommended to use a reverse start–stop mode (inverted configuration) to circumvent high but inefficient conversion rates, because many start-stop cycles never complete while maintaining the time measurement electronics busy. In the reverse mode, the conversion rates are much smaller because they are only as high as the actual photon rates generated by the fluorescence signal. Instrumental response functions of ~25 ps duration can be achieved by using pulsed ps lasers and fast detectors and electronics. The stability of the laser systems and fast and linear response of the electronics permits the recording of very accurate fluorescence decays with a high dynamic range, allowing the determination of lifetimes of the order of 5 ps by using deconvolution (reconvolution) procedures for decay curve analysis[34,35]:

$$I(t) = \int_0^t L(\theta)\, I^{\delta}(t-\theta)\, \mathrm{d}\theta \qquad (1)$$

where the experimental fluorescence decay curve $I(t)$ is a convolution of the instrumental response function (or excitation pulse profile) $L(t)$ with the fluorescence decay $I^{\delta}(t)$ that would be obtained for a δ-pulse of excitation light.

DECAY DATA ANALYSIS

After the latex film containing donor- and acceptor-labeled particles has been annealed at temperatures above T_g, for a period of time t_{diff}, one measures the donor fluorescence decay curve, $I_{DA}(t)$. One of two different strategies can then be followed. For an in-depth characterization of the film morphology, a detailed FRET model has to be used to analyze the donor fluorescence decay curve.[33] Here, we describe a less complex strategy that can be used to evaluate the evolution of interdiffusion as the latex film is formed. In this case, one calculates the quantum efficiency of energy transfer:

$$\Phi_{ET}(t_{diff}) = 1 - \frac{\int_0^{\infty} I_{DA}(t)\, dt}{\int_0^{\infty} I_D(t)\, dt} \qquad (2)$$

where the integrals correspond to the areas under the donor decay curve of a latex film containing mixed donor- and acceptor-labeled particles, $I_{DA}(t)$, and of a latex film containing only donor-labeled particles, $I_D(t)$. This methodology circumvents many disadvantages of the determination of FRET

efficiencies from the fluorescence spectra. Indeed, in this case it is not required that only the donors absorb the excitation light, because the donor decay is invariant to the presence or absence of excited acceptors. Furthermore, since the decays are normalized, the films containing only donors or a mixture of donors and acceptors do not need to have exactly the same optical density. Additionally, geometric effects that are important in steady state fluorescence measurements do not affect the decay curves, and light scattering can be easily removed from the decay curve (although not from the fluorescence spectra).

Although the integral of the donor decay curve of a latex film containing only donor-labeled particles can be easily calculated (it corresponds to the donor decay lifetime, τ_D), to calculate the integral of the donor decay curve measured for the latex film containing mixed donor- and acceptor-labeled particles, it is better to fit the experimental decay using the empirical equation[3,15,36]:

$$I_{DA}(t) = A_1 \exp(-t/\tau_D - P(t/\tau_D)^{1/2} + A_2 \exp(-t/\tau_D) \quad (3)$$

where the term with pre-exponential factor A_1 accounts for the donors that are involved in the energy transfer process, and A_2 is proportional to the amount of donors isolated from acceptors, which decay with the intrinsic lifetime τ_D.

The evolution of the extent of mixing in the latex film as it anneals can then be approximately calculated as the increase in the quantum efficiency of energy transfer, normalized with the values obtained for the film before annealing ($t_{diff} = 0$) and for the fully mixed film ($t_{diff} = \infty$)[28]:

$$f_m(t_{diff}) \approx \frac{\Phi_{ET}(t_{diff}) - \Phi_{ET}(0)}{\Phi_{ET}(\infty) - \Phi_{ET}(0)} \quad (4)$$

The quantum efficiency of energy transfer for the fully mixed film ($t_{diff} = \infty$) can usually be determined by casting a film from a good solvent for the polymer (usually, THF). In cases where the particles are partially crosslinked and complete mixing is not experimentally accessible, it is necessary to estimate this value.[24,37]

The value obtained from equation (4) is a reasonable approximation of the real extent of mixing in the latex film up to about 70% mixing[28]; however, it can generally be used to evaluate the evolution of the extent of mixing. If one needs a more accurate estimate of the extent of mixing, a more complex procedure must be used which details the morphology of the evolving interparticle boundary during film formation.[19,28,30,31,33]

Ideally, the parameter to measure the polymer diffusion rate would be the center-of-mass diffusion coefficient, D_{cm}. For a system as complex as a latex film in which the polymers are initially confined in the deformed particles and have a broad distribution of molecular weights, calculating the distribution of D_{cm} values that characterize the system would be impractical. Instead, it is usual to calculate a single mean diffusion coefficient to describe the diffusion of a polymer characterized by a distribution of diffusivities. The concentration profile of the polymer in a particle can be described as a function of the extent of mixing between the polymer chains from neighboring particles, assuming that the general shape of the polymer segment distribution can be described by Fickian diffusion profile for spherical geometry,[38] for which the donor concentration profiles, $g_D(r)$, is:

$$g_D(r) = \frac{1}{2}\left(erf\left(\frac{R_s + r}{\theta}\right) + erf\left(\frac{R_s - r}{\theta}\right) + \frac{\theta}{\sqrt{\pi} r}\left\{ \exp\left[1 - \left(\frac{R_s + r}{\theta}\right)^2\right] - \exp\left[-\left(\frac{R_s - r}{\theta}\right)^2\right]\right\}\right) \quad (5)$$

where $\theta = 2\sqrt{\langle D \rangle t_{diff}}$ is a parameter measuring the extent of diffusion during a period of time t_{diff}, with average diffusion coefficient <D>, R_s is the radius of the particle, and *erf(z)* is the error function. From the distribution profile we can calculate the volume fraction of polymer mixing f_s:

$$f_s = 1 - \frac{3}{4\pi R_s^3} \int_0^{R_s} 4\pi r^2 g_D(r) dr \quad (6)$$

To calculate the polymer diffusion coefficient during film formation, one then assumes that the normalized increase in the quantum efficiency of energy transfer $f_m(t_{diff})$ is a good estimate of the mass that diffuses across the interparticle boundary $f_s(t_{diff})$.

APPLICATION EXAMPLES

Latex Film Formation

In this example, we monitor the polymer diffusion in poly(butyl methacrylate) latex films with a polymer molar mass of $M_w \approx 125{,}000$ ($M_w/M_n = 2.5$), using polymer nanoparticles labeled with phenantrene (Phe), a FRET donor, and others labeled with 4-dimethylamino-benzophenone (NBen), a nonfluorescent FRET acceptor (*Figure* 3).[14] The dyes were incorporated as (9-phenanthyl)-methyl methacrylate (PheMMA) and 4'-Dimethylamino-2-acryloxy-5-methyl-benzephenone (NBen)[39,40] into a PBMA latex by a two-step seeded emulsion polymerization.

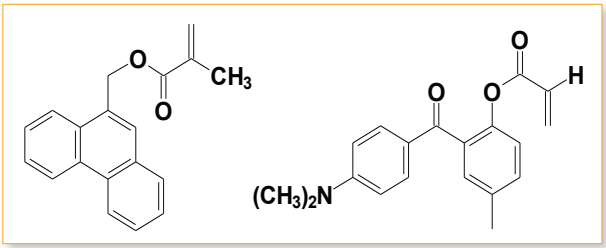

Figure 3—Fluorescent monomers (9-phenanthyl)-methyl methacrylate (Phe, *left*) and 4'-Dimethylamino-2-acryloxy-5-methyl-benzephenone (NBen, *right*).

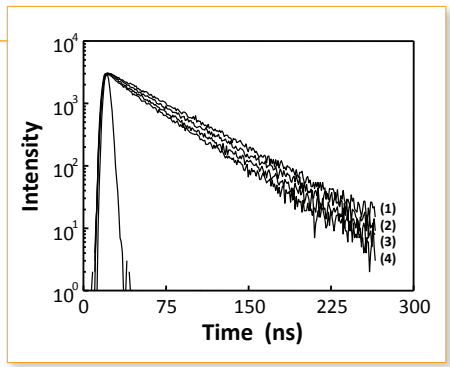

Figure 4—Phenanthrene fluorescence decay profiles in PBMA latex films prepared from Phe-PBMA latex (1) and from a 1:1 ratio of Phe-PBMA and NBen-PBMA lattices (2-4), for a nascent film formed at room temperature (2), a film annealed for 60 min at 90°C (3), and a solvent-cast film (4).

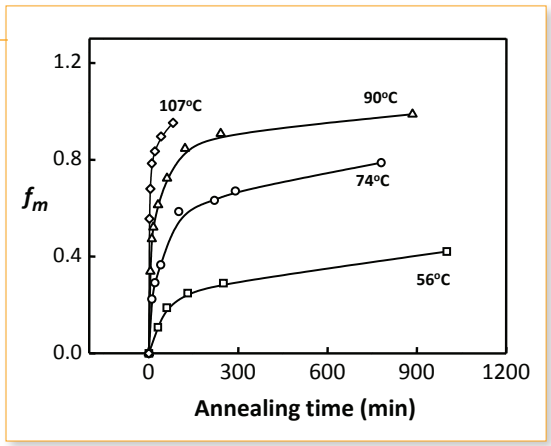

Figure 5—Plots of f_m vs annealing time at different temperatures (56, 74, 90, 107°C) for latex films consisting of 1:1 ratio of Phe-PBMA and NBen(0.3)-PBMA latex particles.

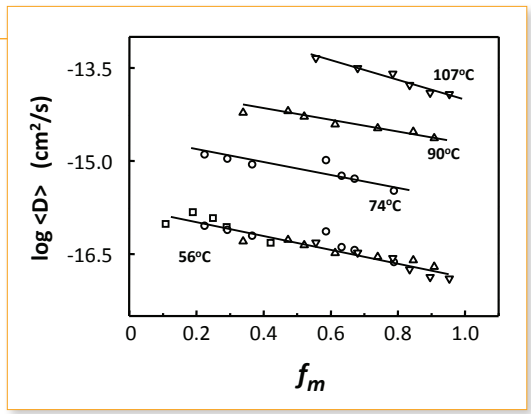

Figure 6—Apparent diffusion coefficient D_{app} vs the extent of mixing f_m at four temperatures (56, 74, 90, and 107 °C). The lowermost curve is a master curve of D_{app} values at 56°C constructed from all of the data using the value of E_a = 34 ± 3 kcal/mol (obtained from experimental data at 56°C).

The latex dispersions were prepared by seeded semicontinuous emulsion polymerization.[14] Latex films were prepared from dispersion mixtures of 1:1 weight ratio of Phe- and NBen-labeled particles. The dispersions were first cleaned with an ion-exchange resin (AG-501-X8 mixed-bed-resin, Bio-Rad) to remove the ionic surfactant and other ionic species before film formation. A few drops of a latex dispersion (containing 1:1 ratio of mixed Phe- and NBen-labeled particle, 6 wt% solids) were spread on a small quartz plate. The film was allowed to dry at room temperature in the open air for one night before annealing. Films were dry and transparent.

The fluorescence decay profiles were measured by the single photon timing technique[34] at room temperature. Phenanthrene was excited at 300 nm, and its emission was recorded over the range 350–400 nm. A band-pass filter (310–400 nm) and a cut-off filter (335 nm) were mounted in the front of the photomultiplier tube detector to minimize the interference due to scattered light. For fluorescence decay measurements, each sample was placed in a small quartz tube and degassed with flowing N_2 for 5 min before each measurement. In Phe(1%)-PBMA latex films (no NBen energy transfer acceptor), Phe decay profiles were fitted with an exponential function, with lifetime τ_D = 46.1 ns.

Polymer diffusion in latex films annealed at 56, 74, 90, and 107 °C was evaluated from the energy transfer quantum efficiency, by approximating the fractional mass that diffused across the particle boundary f_s by the normalized energy transfer quantum efficiency f_m, and calculating the mean apparent diffusion coefficient, D_{app}.

In *Figure* 4, examples of Phe fluorescence decay curves in films prepared from mixed dispersions of Phe(1%)-PBMA and NBen(0.3%)-PBMA are presented. The top curve (1) is the exponential decay from a film prepared from the Phe-PBMA latex only; the curve below (2) shows the small degree of curvature associated with a freshly prepared film obtained from a 1:1 mixture of the donor- and acceptor-labeled latex; the next curve (3) corresponds to the same film after it was annealed for 60 min at 90°C; and the bottom curve (4) was obtained for a solvent-cast film, representing full mixing of the donor- and acceptor-labeled polymer.

From the decay curves in *Figure* 4, we calculate energy transfer quantum efficiencies of Φ_{ET} = 0.07 for the newly formed film and Φ_{ET} = 0.37 for the solvent-cast film, using equation (2). Values of f_m calculated from equation (4) are presented in *Figure* 5 for a film annealed at four different temperatures. One can see that the annealing temperature has a large effect on the rate of polymer diffusion, with f_m increasing to 1

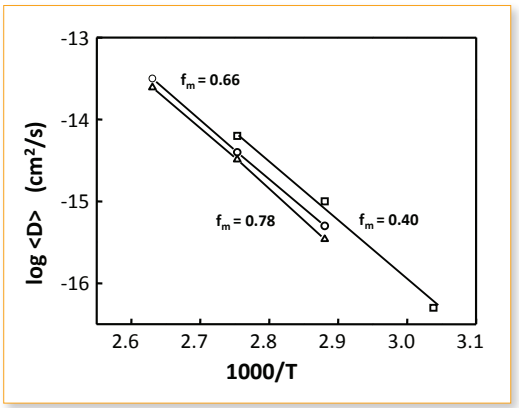

Figure 7—Arrhenius plot of log D_{app} for f_m values 0.40, 0.66, and 0.78 (top to bottom).

in only a few minutes at 107°C, but reaching only 0.4 after annealing 15 hr at 56°C.

D_{app} values calculated in this way for the data in *Figure* 5 are plotted against f_m in *Figure* 6. These values increase markedly with increasing temperature. There is also a tendency for these values to decrease with increasing f_m, which we attribute to the molecular weight polydispersity of our latex samples.

In *Figure* 7, the D_{app} values obtained at different temperatures are plotted in an Arrhenius fashion. In making these plots, we compare D_{app} values at similar extents of mixing. For three different values of f_m, these data can be fitted with an apparent activation energy E_a = 34 ± 3 kcal/mol. To emphasize the fact that this value pertains to all the data, we use this value to calculate a shift factor to create a master curve of D_{app} values at 56°C (*Figure* 6).

Reactive Latex Blends

In this example, FRET is used to evaluate a reactive blend in which the two components have initially limited miscibility, but become miscible as the reaction proceeds.[41] In this type of system, the growth in the quantum efficiency of energy transfer f_m allows one to monitor both the rate of polymer diffusion across the interparticle boundary and how this rate is affected by the chemical reaction.

Poly(ethylhexyl methacrylate) (PEHMA) latex particles containing reactive functional groups, either 11 mol% methacrylic acid (MAA) or 5 mol% t-butylcarbodiimidoethyl methacrylate (tBCEMA),[42] and labeled with either 9-phenanthrylmethyl methacrylate or 9-anthryl methacrylate,[43] were prepared by a two-stage emulsion polymerization from a common seed under monomer-starved conditions. Phenanthrene-labeled PEHMA latex (Phe-PEHMA), phenanthrene-labeled carboxylic acid-containing PEHMA latex (Phe-PEHMAA-MAA), anthracene-labeled PEHMA latex (Ant-PEHMA) and anthracene-

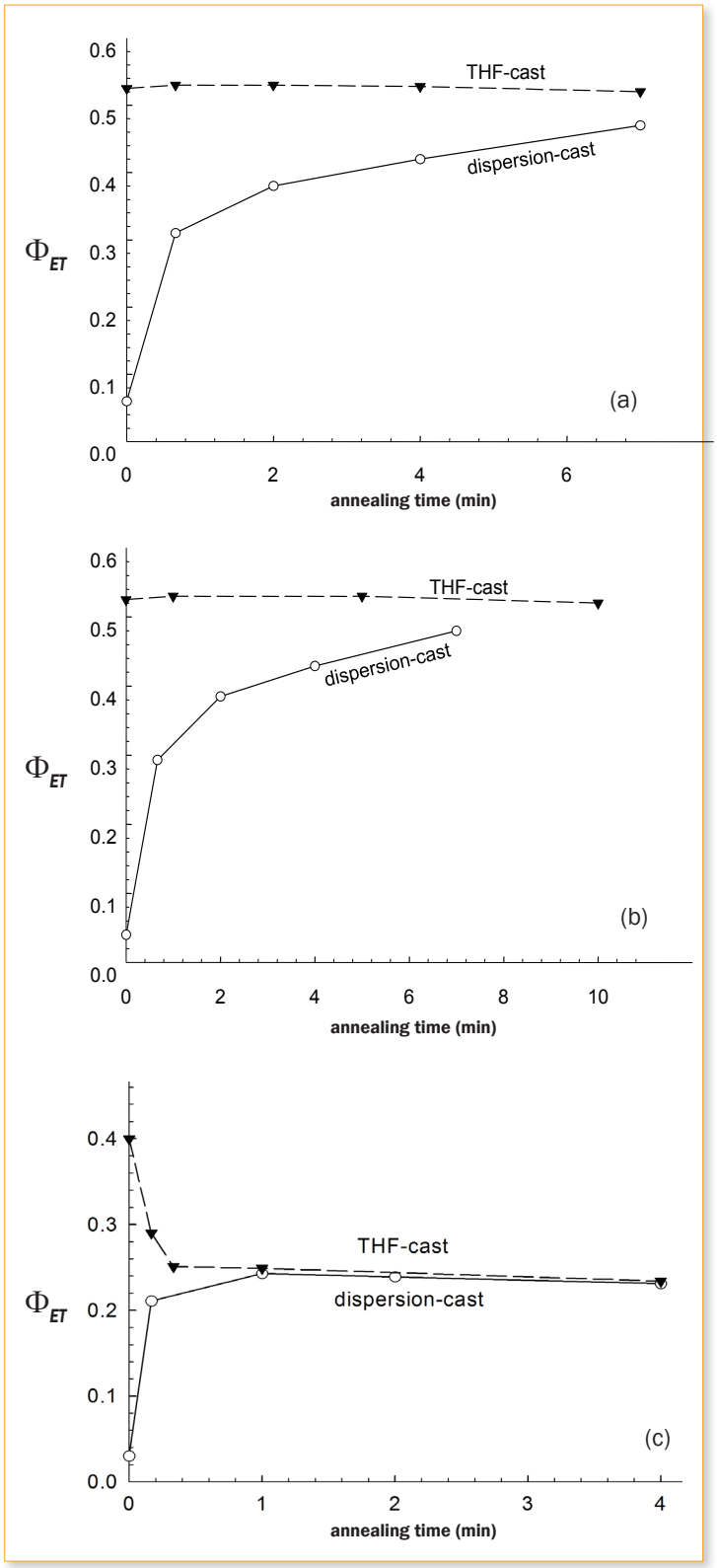

Figure 8—Evolution of Φ_{ET} with annealing time in dispersion-cast and THF-cast films prepared from (a) Phe-PEHMA / Ant-PEHMA; (b) Phe-PEHMA / Ant-PEHMA-tBCEMA; and (c) Phe-PEHMA-MAA / Ant-PEHMA blends, annealed at 60°C.

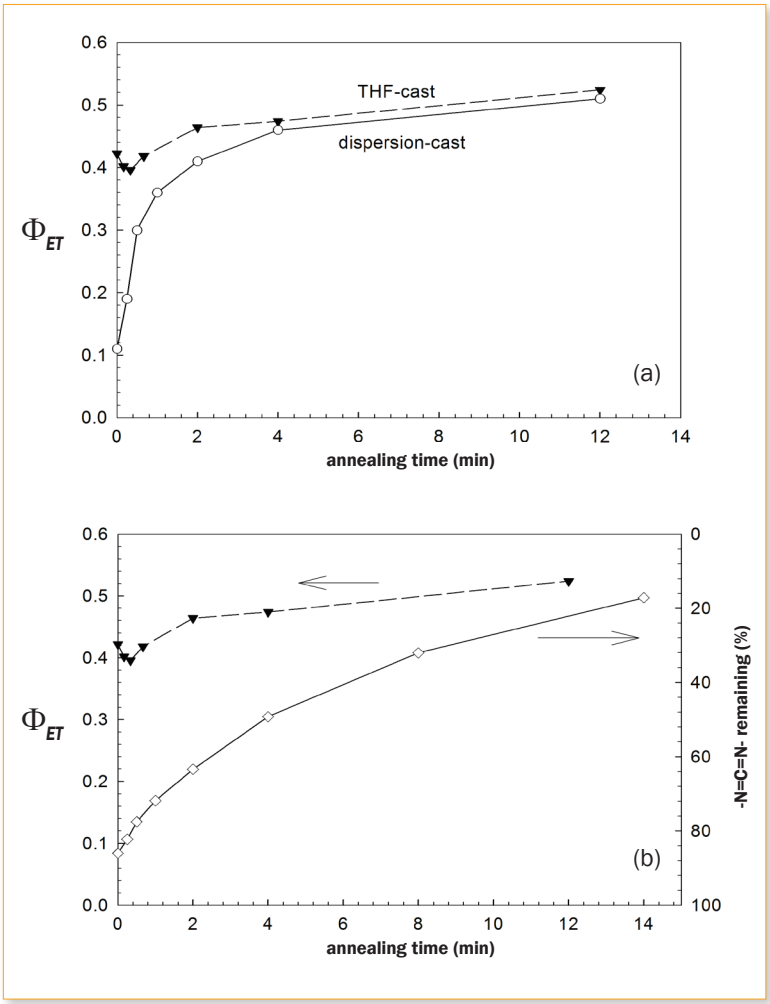

Figure 9—Evolution of Φ_{ET} (a) and remaining -N=C=N- groups (b) with annealing time in THF-cast films prepared from a blend of Phe-PEHMA-MAA/Ant-PEHMA-tBCEMA annealed at 60°C.

labeled tBCEMA-containing PEHMA latex (Ant-PEHMAA-tBCEMA) were prepared with 1 mol% of fluorescent dyes.

Films prepared from a 1:1 mixture of Phe-PEHMA and Ant-PEHMA—one cast directly from the latex dispersion at 4°C, and the other cast from a THF solution prepared from the freeze-dried latex mixture—yield Φ_{ET} = 0.06 and Φ_{ET} = 0.52, respectively. When the same films are annealed at 60°C, Φ_{ET} remains at 0.52 ± 0.01 for the THF-cast film and increases to 0.49 (in 12 min) for the dispersion-cast film. In the last case, the polymers diffuse across the interparticle boundary, bringing the Phe and An groups into proximity and increasing Φ_{ET} (*Figure* 8a). The fact that the maximum value of Φ_{ET} obtained for the dispersion-cast film corresponds to that obtained for (homogeneous) films cast from THF indicates that the polymers are fully miscible.

For dispersion-cast and THF-cast films prepared from a blend of Phe-PEHMA and Ant-PEHMA-tBCEMA (*Figure* 8b), Φ_{ET} behaves in a similar way to the blend of Phe-PEHMA and Ant-PEHMA (*Figure* 8a), yielding Φ_{ET} = 0.52 for the THF-cast films, and Φ_{ET} increasing to 0.52 upon annealing for the dispersion-cast films. This indicates that Ant-PEHMA-tBCEMA and Phe-PEHMA are also miscible.

However, the presence of 11 mol% MAA units in the PEHMA-MAA latex is sufficient to induce phase separation when this polymer is blended with PEHMA (*Figure* 8c). The limited miscibility of these polymers would not be apparent by traditional methods since the blends of PEHMA with PEHMA-MAA are transparent, and the T_g of the two components are too close for the presence of separate phases to be detected by differential scanning calorimetry or dynamic mechanical measurements. In this blend, Φ_{ET} increases much slower and only to 0.24 in dispersion-cast films annealed at 60°C, while for solvent-cast films, Φ_{ET} decreases from 0.40 (less than full mixing) to 0.23, upon annealing at 60 °C. This indicates that further demixing takes place, leading to increased separation of the Phe- and An-labeled polymers.

The mixture of PEHMA lattices containing 11 mol% MAA and 5 mol% tBCEMA, Phe-PEHMA-MAA and Ant-PEHMA-tBCEMA yields a reactive blend in which the two polymers contain functional groups that can combine to produce a graft copolymer, eventually evolving to a crosslinked network. The extent of polymer interdiffusion can be followed by FRET, while the extent of chemical reaction is traced by Fourier transform infrared spectroscopy (FTIR), taking advantage of the carbodiimide band at 2128 cm^{-1}.[44]

The dispersion-cast film exhibits polymer segregation that persists in the solid film when this is annealed for short times at 60°C. However, over longer times, mixing does occur, and reaches completion (*Figure* 9a). The growth in polymer miscibility is coupled to the reaction between the carboxylic (-COOH) and carbodiimide (-N=C=N-) groups of MAA and tBCEMA to form an N-acyl urea,[45] creating a covalent bond between the two polymers in the process. Polymer diffusion is necessary to bring the reactive groups together, but the chemical reaction introduces branches into the polymer. On one hand, the branches compatibilize the blend, but on the other hand, they retard the diffusion, creating crosslinks that bring polymer diffusion to a halt.

In the newly formed THF-cast film, Φ_{ET} = 0.42, a value that indicates some segregation. By annealing at 60°C, Φ_{ET} decreases to 0.40 over the first 20 min due to demixing of the polymers. However, for longer annealing times, Φ_{ET} increases due to mixing promoted by the reaction between -N=C=N- and -COOH groups, with Φ_{ET} reaching 0.52 (fully mixed film). The state of mixing (from

Φ_{ET}) correlates very well with the extent of carbodiimide reaction monitored by the decrease in the FTIR intensity at 2128 cm^{-1} (*Figure* 9b).

The combined action of polymer diffusion and anchoring by the *N*-acyl urea overcomes the mixibility problem of the two blend components and results in a film with good mechanical properties.

CONCLUSION

Fluorescence decay methods allow very precise evaluation of FRET efficiency in polymer films labeled with appropriate donor and acceptor dyes. This technique has been extensively used in the characterization of latex film formation in different systems, such as thermosets, blends, reactive blends, etc. By allowing the measurement of polymer chain diffusion in the films at the nanometer scale, FRET can be used to quantify the extent of mixing between polymer chains from different particles, which ultimately leads to the formation of a coating with good mechanical properties.

ACKNOWLEDGMENTS

We acknowledge the support of FCT (Portugal) and POCI 2010 (FEDER), projects PTDC/CTM-NAN/115110/2009 and PEst-OE/CTM/LA0024/2011.

References

1. Keddie, J.L. and Routh, A.F., *Fundamentals of Latex Film Formation: Processes and Properties,* Springer, UK, 2010.
2. Wang Y.C. and Winnik, M.A., *J. Phys. Chem.,* 97, 2507 (1993).
3. Winnik, M.A., Wang, Y.C., and Haley, F., "Latex Film Formation at the Molecular Level: The Effect of Coalescing Aids on Polymer Diffusion," *J. Coat. Technol.,* 64, No. 815, 51 (1992).
4. Geoghegan, M., Jones, R.A.L., Sivia, D.S., Penfold, J., and Clough A.S., *Phys. Rev. E,* 53, 825 (1996).
5. Hahn, K., Ley, G., and Oberthur, R., *Colloid Polym. Sci.,* 266, 631(1988).
6. Hahn, K., Ley, G., Schuller, H., and Oberthur, R., *Colloid Polym. Sci.,* 264, 1092 (1986).
7. Yoo, J.N., Sperling, L.H., Glinka, C.J., and Klein, A., *Macromolecules*, 23, 3962 (1990); 24, 2868 (1991).
8. Morawetz, H., *Science,* 203, 405 (1979).
9. Morawetz, H., *Science,* 240, 172 (1988).
10. Morawetz, H., *J. Polym. Sci. Part A: Polym. Chem.,* 37, 1725 (1999).
11. Winnik, M.A., *Current Opinion in Colloid & Interface Science,* 2, 192 (1997).
12. Taylor, J.W. and Winnik, M.A., "Functional Latex and Thermoset Latex Films," *J. Coat. Technol. Res.,* 1, No. 3, 163 (2004).
13. Wang, Y.C., Zhao, C.L., and Winnik, M.A., *J. Chem. Phys.*, 95, 2143 (1991).
14. Ye, X., Farinha, J.P.S., Oh, J.K.,Winnik, M.A., and Wu, C., *Macromolecules*, 36, 8749 (2003).
15. Wang, Y. and Winnik, M.A., *J. Phys. Chem.,* 97, 2507 (1993).
16. Feng, J. and Winnik, M.A., *Macromolecules*, 30, 4324 (1997).
17. Kawaguchi, S., Odrobina, E., and Winnik, M.A., *Macromol. Rapid Commun*., 16, 86 (1995).
18. Juhué, D., Wang, Y.C., and Winnik, M.A., *Makromol. Chem. Rapid Commun.,* 14, 345 (1993).
19. Farinha, J.P.S., Martinho, J.M.G. , Kawaguchi, S.K., Yekta, A., and Winnik, M.A., *J. Phys. Chem.*, 100 (30), 12552 (1996).
20. (a) Kim, H.B. and Winnik, M.A., *Macromolecules*, 27, 1007 (1994); (b) Kim, H.B. and Winnik, M.A., *Macromolecules*, 28, 2033 (1995).
21. Tsutomu, M., Koji, A., Masatoshi, M., and Yoshiharu K., *Prog. Org. Coat.*, 55, 276 (2006).
22. Mitsuru, K., Yahya, R., Laurent, B., Lan, C., and Winnik, M.A., *Macromolecules*, 35, 7387 (2002).
23. Mitsuru W. and Toshiyuki, T., *J. Polym. Sci. Part A: Polym. Chem.*, 44, 4736 (2006).
24. Ribeiro, T., Fedorov, A., Baleizão, C., and Farinha, J.P.S., *J. Colloid Interface Sci.,* 401, 14 (2013).
25. Baumann, J. and Fayer, M.D., *J. Chem. Phys.*, 85, 4087 (1986).
26. Klafter, J. and Blumen, A., *J. Chem. Phys.*, 80, 875 (1984).
27. Drake, J.M., Klafter, J., and Levitz, P., *Science*, 25 (5001), 1574 (1991).
28. Farinha, J.P.S., Martinho, J.M.G.; Yekta, A., and Winnik, M. A., *Macromolecules,* 28, 6084 (1995).
29. Yekta, A., Duhamel, J., and Winnik, M.A., *Chem. Phys. Letters,* 235, 119 (1995).
30. Farinha, J.P.S. and Martinho, J.M.G., *J. Luminescence*, 72, 914 (1997).
31. Yekta, A., Winnik, M.A., Farinha, J.P.S., and Martinho J. M.G., *J. Phys. Chem. A*, 101, 1787 (1997).
32. Farinha, J.P.S., Spiro, J.G., and Winnik, M.A., *J. Phys. Chem. B*, 108 (42), 16392 (2004).
33. Martinho, J.M.G. and Farinha, J.P.S., *J. Phys. Chem. C* 112, 1059 (2008).
34. O'Connor, D.V. and Phillips, D., *Time-Correlated Single Photon Counting*, Academic Press: London, UK, 1984.
35. Farinha, J.P.S., Martinho, J.M.G., and Pogliani, L., *J. Math. Chem.*, 21, 13 (1997).
36. Wang, Y.C., Zhao, C.L., and Winnik, M.A., *J. Chem. Phys.* 95, 2143 (1991).
37. Piçarra, S., Afonso, C.A.M., Kutreva, V.B., Fedorov, A., Martinho, J. M.G. and Farinha, J.P. S., *J. Colloid Interface Sci.* 368, 2 (2012).
38. Crank, J., *The Mathematics of Diffusion*, Clarendon: Oxford, 1975.
39. Oh, J. K., Wu, J., Winnik, M.A., Craun, G.P., Rademacher, J., and Farwaha, R., *J. Poly. Sci. Part A. Polym. Chem.*, 40, 1594 (2002).
40. Oh, J.K., Wu, J., Winnik, M.A., Craun, G.P., Rademacher, J., and Farwaha, R., *J. Poly. Sci. Part A. Polym. Chem.*, 40, 300 (2002).
41. Pham, H., Farinha, J.P.S., and Winnik, M.A., *Macromolecules*, 33, 5850 (2000).
42. Pham, H.H. and Winnik, M.A., *J. Polym. Sci. Part A: Polym. Chem.,* 38, 855 (2000).
43. Feng, J., Ph. D. Thesis, University of Toronto, 1998.
44. Dolphin, D. and Wick, A., *Tabulation of Infrared Spectral Data,* Wiley-Interscience, 1977.
45. Taylor, J.W. and Bassett, D.R., *ACS Symposium Series*, 663, 137 (1997).

AUTHORS

J.M.G. Martinho and **J.P.S. Farinha**, CQFM (Centro de Química-Física Molecular) and Institute of Nanoscience and Nanotechnology (IN), Instituto Superior Técnico, 1049-001 Lisboa, Portugal; jgmartinho@ist.utl.pt and farinha@ist.utl.pt.